Resting $CMRO_2$ fluctuations show persistent network hyper-connectivity following exposure to sub-concussive collisions

Allen A. Champagne[a], Nicole S. Coverdale[a], Joseph Y. Nashed[a], Juan Fernandez-Ruiz[b], Douglas J. Cook[a,c,*]

[a] Centre for Neuroscience Studies, Room 260, Queen's University, Kingston, ON K7L 3N6, Canada
[b] Departamento de Fisiología, Facultad de Medicina, Universidad Nacional Autónoma de México, Av. Universidad 3000, Coyoacán, Ciudad de México 04510, México
[c] Department of Surgery, Queen's University, Room 232, 18 Stuart St, Kingston, ON K7L 3N6, Canada

ABSTRACT

Exposure to head impacts may alter brain connectivity within cortical hubs such as the default-mode network (DMN). However, studies have yet to consider the confounding effects of altered resting cerebral blood flow (CBF_0) and cerebrovascular reactivity (CVR) on changes in connectivity following sub-concussive impacts. Here, 23 Canadian collegiate football players were followed during a season using calibrated resting-state MRI and helmet accelerometers to examine the interplay between the neural and vascular factors that determine functional connectivity (FC). Connectivity-based analyses using blood oxygen level dependent (BOLD) and cerebral metabolic rate of oxygen consumption ($CMRO_2$) mapping were used to study the DMN longitudinally. Network-specific decreases in CBF_0 were observed one month following the season, while impaired CVR was documented at both mid-season and one month following the season, compared to pre-season baseline. Alterations in CBF_0 and BOLD-based CVR throughout the season suggest that neurophysiological markers may show different susceptibility timelines following head impacts. DMN connectivity was increased throughout the season, independent of changes in cerebrovascular physiology, suggesting that alterations in FC following sub-concussive impacts are robust and independent of changes in brain hemodynamics. No significant correlations between impact kinematics and DMN connectivity changes were documented in this study. Altogether, these findings create a strong paradigm for future studies to examine the underlying neural and vascular mechanisms associated with increases in network connectivity following repeated exposure to sub-concussive collisions, in an effort to improve management of head impacts in contact sports.

1. Introduction

Over the course of a season, collegiate football players experience a large number of head impacts that are sub-concussive (Broglio et al., 2011; Reynolds et al., 2017a). Sub-concussive impacts are defined as impacts that do not cause the array of symptoms typically associated with sport-related concussion (SRC; Mccrea et al., 2003; McCrory et al., 2013; Nelson et al., 2013). In recent years, the acute and chronic effects of repeated exposure to sub-concussive impacts has raised concern within the sport community (Findler, 2015; Omalu, 2015; Sanders, 2016). In general, these concern are driven by the fact that cumulative exposure (Montenigro et al., 2016; Stamm et al., 2015), and SRC history (Churchill et al., 2017; Tremblay et al., 2014), may contribute to functional and structural changes within the brain that are observed

longitudinally in retired professional athletes.

Neuroimaging has emerged as an informative tool to investigate the effects of sub-concussive head trauma on brain functional integrity. One modality of particular interest is resting-state functional magnetic resonance imaging (rs-fMRI), which reflects the degree of synchrony between low-frequency spontaneous fluctuations in the Blood Oxygen Level Dependent (BOLD) signal (Biswal et al., 2007; Cordes et al., 2000; Kannurpatti and Biswal, 2008). Rs-fMRI can be used to examine intrinsic brain activity and coordination across functionally-related but spatially distinct brain regions and quantified as functional connectivity (FC) within the whole-brain (Fox et al., 2005; Shirer et al., 2012), or specific networks of interest (Finn et al., 2015), such as the default mode network (DMN; Greicius et al., 2003, 2009; Uddin et al., 2009). Alterations in BOLD-FC have been documented following season-long

exposure to sub-concussive head impacts (Abbas et al., 2015a, 2015b; Reynolds et al., 2017b; Slobounov et al., 2017), and acute onset participation in a single rugby game (Johnson et al., 2014), suggesting that repetitive head trauma may alter brain network organization, without the presence of a concussion.

In fMRI, BOLD is used as a surrogate for neuronal activity (Ogawa et al., 1990) by way of the relationship between neural activation, local increases in blood flow (due to neurovascular coupling), and subsequent decreases in deoxy-hemoglobin concentration, which lengthens T_2^* relaxation. The functional hyperemia following neuronal activation relates the increase in signal to greater cellular metabolic activity, which can be quantified indirectly using BOLD-based imaging (Davis et al., 1998). During rs-fMRI, spontaneous fluctuations in the BOLD contrast reflect a complex interplay between neural, vascular and metabolic factors, which together, make up the signal used to infer FC measurements (Carusone et al., 2002; Kannurpatti et al., 2010; Liu, 2013; Tak et al., 2014). Though it has been shown that resting-state BOLD fluctuations may partially reflect local metabolic processes in the absence of a stimuli (Fukunaga et al., 2008), studies using BOLD-based rs-fMRI to explore the effects of head impacts on FC have yet to account for the interdependency between the BOLD signal and local fluctuations in perfusion based on neurovascular coupling (Chu et al., 2018; Tak et al., 2015, 2014). This relationship may arise from spurious correlations due to macrovascular drainage routes across the brain (Jo et al., 2010; Tak et al., 2015) or cerebral blood flow (CBF) fluctuations as a function of neuronal activity, and changes in cerebral metabolic rate of oxygenation (CMRO2; Chuang et al., 2008; Fukunaga et al., 2008; Liang et al., 2013; Viviani et al., 2011; Wu et al., 2009; Zou et al., 2009).

This dependency of the BOLD signal on multiple factors is an important limitation given that baseline cerebral blood flow (CBF_0) and cerebrovascular reactivity (CVR) affect the signal (Chu et al., 2018; Li et al., 2014, 2012; Liang et al., 2013; Liu, 2013), and both measures may be altered following exposure to head impacts (Slobounov et al., 2017; Svaldi et al., 2017, 2015). CBF provides an index for the mean delivery of arterial blood to cerebral tissues over time, while CVR reflects the capacity of the arterial blood vessels to alter blood flow in response to a vasoactive stimulus (Mandell et al., 2008; Yezhuvath et al., 2009). Additional research has also shown that in areas with impairments in CVR, there may be an uncoupling between neuronal activation and blood flow, which inherently confounds BOLD-based fMRI (Para et al., 2017), and network BOLD-FC measurements (Tak et al., 2015, 2014). Preliminary changes in FC following exposure to repetitive head trauma (Abbas et al., 2015a, 2015b; Reynolds et al., 2017b; Slobounov et al., 2017) are often interpreted as impairments in neural connectivity (decreased FC), or hyper-connected compensatory mechanisms for neural recruitment (increased FC). However, it is critical that we consider the robust effect of physiological modulators (CBF_0, CVR and CMRO2; Chu et al., 2018; Fukunaga et al., 2008) on the BOLD signal, in order to acheive more informed conclusions regarding the potential changes in network FC following participation in contact sports.

A large volume of studies have provided evidence that the biomechanics of impacts sustained by football players across all sports levels vary between positions (Broglio et al., 2012; Crisco et al., 2012; Crisco et al., 2010, b; Mihalik et al. 2007), session types (i.e. games vs. practices; Mihalik et al. 2007b; Schmidt et al. 2016), starting status (Broglio et al. 2011), and, even based on different offensive strategies (Martini et al. 2013). Changes in impact biomechanics, and rates of head injuries, have also been documented over the course of a season, as generally more SRC (Kerr et al. 2015), and high g-force sub-concussive collisions (Slobounov et al. 2017), are sustained during the first weeks of practice. Despite these findings however, there remains a gap in knowledge about the relationship between sub-concussive impact kinetics and possible changes in network FC.

In this work, we use calibrated resting-state imaging (Wu et al. 2009) to account for physiological modulators related to the BOLD signal, and to investigate the effects of repetitive sub-concussive head impacts on changes in CMRO2-based FC strength. Longitudinal changes in BOLD- and CMRO2-based FC were examined in the DMN, throughout a season of collegiate football, given previous evidence of vulnerability of the DMN following exposure to head impacts (Abbas et al. 2015a, 2015b; Johnson et al. 2014; Reynolds et al. 2017b; Slobounov et al. 2017). Changes in FC over time were correlated with head impact kinematics, based on data acquired using helmet accelerometers, in order to explore the relationship between exposure and changes in network connectivity. We hypothesized that differences in BOLD-based DMN connectivity would be significantly confounded by changes in CBF_0 and CVR throughout the season. Furthermore, we predicted that CMRO2-based correlations would show differences in the strength and spatial distribution of FC following exposure to head impacts, while minimizing the confounding effects of vascular hemodynamics. Finally, we hypothesized that increased exposure to head impacts would be associated with greater changes in network connectivity.

2. Methods

2.1. Subjects and ethical approval

The protocol used in this work was approved by the Queen's University Health Sciences Research Ethics Board (Kingston, ON, Canada) and informed consent was obtained for all participants. In this study, 26 collegiate Canadian football players were enrolled in a longitudinal neuroimaging study (Fig. 1). The first imaging time point was completed at pre-season baseline, within two months before the first contact practice at the start of the training camp ('PRE'). Data from three of these subjects were removed due to anxiety in the magnet bore ($N = 2$), and poor data quality due to excessive motion ($N = 1$). Of the remaining 23 athletes (Table 1), 15 were brought back for neuroimaging after a 14-day training camp period, and the first two season games (post training-camp, 'PTC'). Eight players did not complete the mid-season time point due to SRC ($N = 2$) or season ending injuries ($N = 6$). One month following the last game of the season, 12 athletes completed
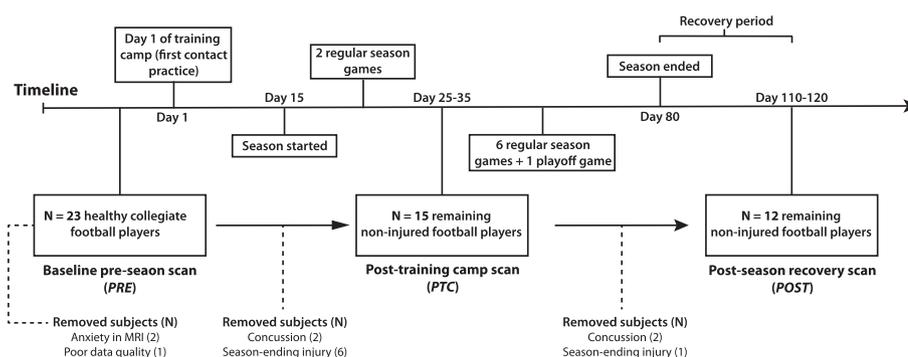
Fig. 1. Schematic timeline of the season, scheduled scan times and removal of subjects. The timeline of the study design shows when football players were scanned; prior to the first contact practice of the season (day 1 of training camp; PRE), following training-camp and two season games (PTC), and one month following the last playoff game of the season (POST). Subjects removed at each time point are illustrated with a dotted line. The number of subjects in bold at each time point were included in the mixed analysis for the effect of time, on each parameter.

Table 1
Subject demographics based on history of sport-concussion.

	No SRC (N = 9)	*Previous SRC (N = 14)*
Age (years)	20 ± 1	21 ± 1
Height (cm)	184 ± 6	185 ± 6
Weight (kg)	99 ± 17	94 ± 6
Number of prior concussions (N)	0	1.4 ± 0.5 (range: 1–2)
Time since injury (years)	N/A	5 ± 3 (range: 2–10)
Position (N)	DB (3)	DB (3)
	DL (2)	DL (1)
	LB (2)	LB (5)
	OL (1)	S (1)
	WR (1)	TE (2)
		WR (2)

Values are mean ± standard deviation unless stated otherwise. DB = defensive back, DL = defensive lineman, LB = linebacker, N/A = not applicable, OL = offensive lineman, S = safety, SRC = sport-related concussion, TE = tight-end, WR = wide-receiver.

the imaging at the final time point (post-season, 'POST') in order to test whether physiological and connectivity-based metrics had returned towards baseline values. This was done because athletes did not engage in any contact activities following the last competitive game of the season, allowing for possible recovery of the changes in imaging markers. The three athletes that did not complete the post-season imaging were removed due to SRC (N = 2) sustained between the PTC and POST time points and a season-ending knee injury (N = 1).

2.2. Characterizing exposure to sub-concussive impacts

All athletes enrolled in this study were required to wear the Riddell Revolution Speed helmet (Riddell, Elyria, OH). Helmets were mounted with gForce tracker accelerometers (gForce Tracker, GFT; Hardware version GFT3S ver4.0, Artaflex Inc., Markham, ON, Canada), which provide in-depth kinematic information about each impact to the head (Fig. 2). The GFT hardware has been validated using laboratory controlled impacts, showing that the system is appropriate for monitoring exposure to head impacts (Campbell et al. 2016). The five impact locations (i.e. 'front', 'top', 'right', 'left' and 'back') were binned based on information about elevation and azimuth angle, similar to Mihalik et al. (2007). The minimum peak linear acceleration for collection was set to 15 g, to align with previously published literature using the same technology (Campbell et al. 2016).

A total of three impact kinematic features were used to characterize exposure for each player. These included the total hit count, the mean linear acceleration (g) and the mean rotational velocity (°/s), averaged on a per session basis, as an index for the daily exposure that each athlete sustained between the PRE and PTC time points. Only these impacts were used in the linear regression analyses of the neuroimaging data between the PRE and PTC time points to study the acute effects of sub-concussive impacts.

2.3. Structural imaging and tissue segmentation

Imaging data were collected from all subjects on a Siemens 3.0 T Magnetom Tim Trio system using a 32-channel head coil receiver. An anatomical T_1-weighted MP-RAGE (magnetization prepared rapid acquisition gradient echo) was acquired for accurate segmentation and registration into standard space using the following parameters: TR = 1760 ms, TE = 2.2 ms, time of inversion (TI) = 900 ms, voxel size = 1 mm isotropic, field of view (FOV) = 256 × 256 mm, flip angle = 9°, receiver bandwidth = 200 Hz/pixel. Subject-specific grey-matter (GM), white-matter (WM) and cerebrospinal fluid (CSF) maps were generated for each subject using 3D automatic segmentation (FAST) (Zhang et al. 2001). The T_1 and tissue maps were then spatially resampled onto the Montreal Neurological Institute (MNI) standard

template (2-mm isotropic) using affine (12 DOF) (Jenkinson et al. 2002), and non-linear warp-fields (FNIRT; Andersson et al. 2007).

2.4. Dual-echo resting-state fMRI and pre-processing

To derive $CMRO_2$ fluctuations, resting-state BOLD and perfusion data were acquired simultaneously using a dual-echo pseudo-continuous arterial spin labeling sequence (pCASL; Alsop et al. 2015; Dai et al. 2008) with echo planar imaging (EPI) readout: TR = 4000 ms, TE_1/TE_2 = 10/30 ms, FOV = 250 × 250 mm, flip angle = 90°, voxel size = 3.9 mm isotropic, post-labeling delay (PLD) = 1000 ms, slice gap = 0.773 mm, label offset = 100 mm, receiver bandwidth = 2604 Hz/pixel, EPI factor = 64, tagging duration 1.665 s (Wu et al. 2007). A total of 25 axial slices were acquired on a 64 × 64 matrix (7/8 partial Fourier) in ascending order for whole brain coverage using parallel imaging (GRAPPA acceleration factor = 2). During the RS scan (9 min), subjects were instructed to keep their eyes open, focus on a fixation cross, and remain awake. EPI images were calibrated using a pre-scan normalized image acquired using the body transmit/receiver coil, which corrects for inhomogeneities in the receive sensitivity of the 32-channel head coil.

RS data were preprocessed using a combination of FSL (Jenkinson et al. 2012), AFNI (Cox 1996) and in-house designed Matlab (MATLAB 2015b, The MathWorks, Inc., Natick, Massachusetts, United States) scripts (Fig. 3A). After discarding the first two volumes to ensure MR steady state, both echoes were split and motion corrected using FSL's MCFLIRT and the first volume as the reference template (Jenkinson et al. 2002; Jenkinson and Bannister, 2002). Once re-aligned, the volumes were averaged over time to extract non-brain tissues using the brain extraction tool (BET). The BOLD data were then reconstructed using a surround averaging of the second echo (TE = 30 ms) and low-pass filtered at half the Nyquist frequency (i.e. 1/4TR; Tak et al., 2014, 2015). The ASL data (TE = 10 ms) were high-pass filtered with a cutoff frequency of 1/4TR to remove low-frequency BOLD contamination. All BOLD and ASL time frames were spatially transformed into MNI space (2-mm isotropic) via the structural scans, using boundary-based registration (Greve and Fischl 2009), and spatially smoothed using a 8 mm full-width at half-maximum (FWHM) Gaussian kernel. As described in Tak et al. 2014 (Tak et al. 2014), the CBF weighted image contains some T_2^* weighting from the BOLD effect, which must be removed to avoid BOLD contamination of the ASL signal. Following steps introduced by (Chuang et al. 2008), and others (Nasrallah et al. 2012; Wu et al. 2009; Zou et al. 2009), the ASL signal was demodulated to the low frequency range by multiplying each volume by cos[πn] where n denotes the volume number (see Fig. 2 in Tak et al. 2014). In this analysis, cardiac and respiratory contribution to the signal were assumed to be global across the brain, although these can also vary across the head (Brosch et al. 2002; Van de Moortele et al. 2002). Since neuronal activity-related signal in the WM and CSF is minimal, the segmented tissues were used as regions-of-interest (ROIs) to remove cardiac and respiratory noise. Signal from WM and CSF ROIs, along with the 6 standard motion parameters were used to clean the resampled resting data using FSL's regfilt tool (Jenkinson et al. 2012).

2.5. Calibrated fMRI and voxelwise computation of M

In calibrated fMRI, the M parameter represents the voxelwise calibration value needed to derive the $CMRO_2$ signal (see below; Davis et al. 1998; Hoge et al. 1999). To estimate voxelwise M maps, each subject completed a 6-min hypercapnia (HC) and hyperoxia (HO) step protocols with dual-echo pCASL (Alsop et al. 2015; Dai et al. 2008) imaging and the same parameters described above. For quantification of CBF, a tissue equilibrium magnetization map (M_0) was also acquired using a longer TR (15,000 ms) and no spin labelling. BOLD data were isolated from the pCASL timeseries using a surround averaging of the second echo (TE = 30 ms; Smith and Brady 1997), while the ASL were
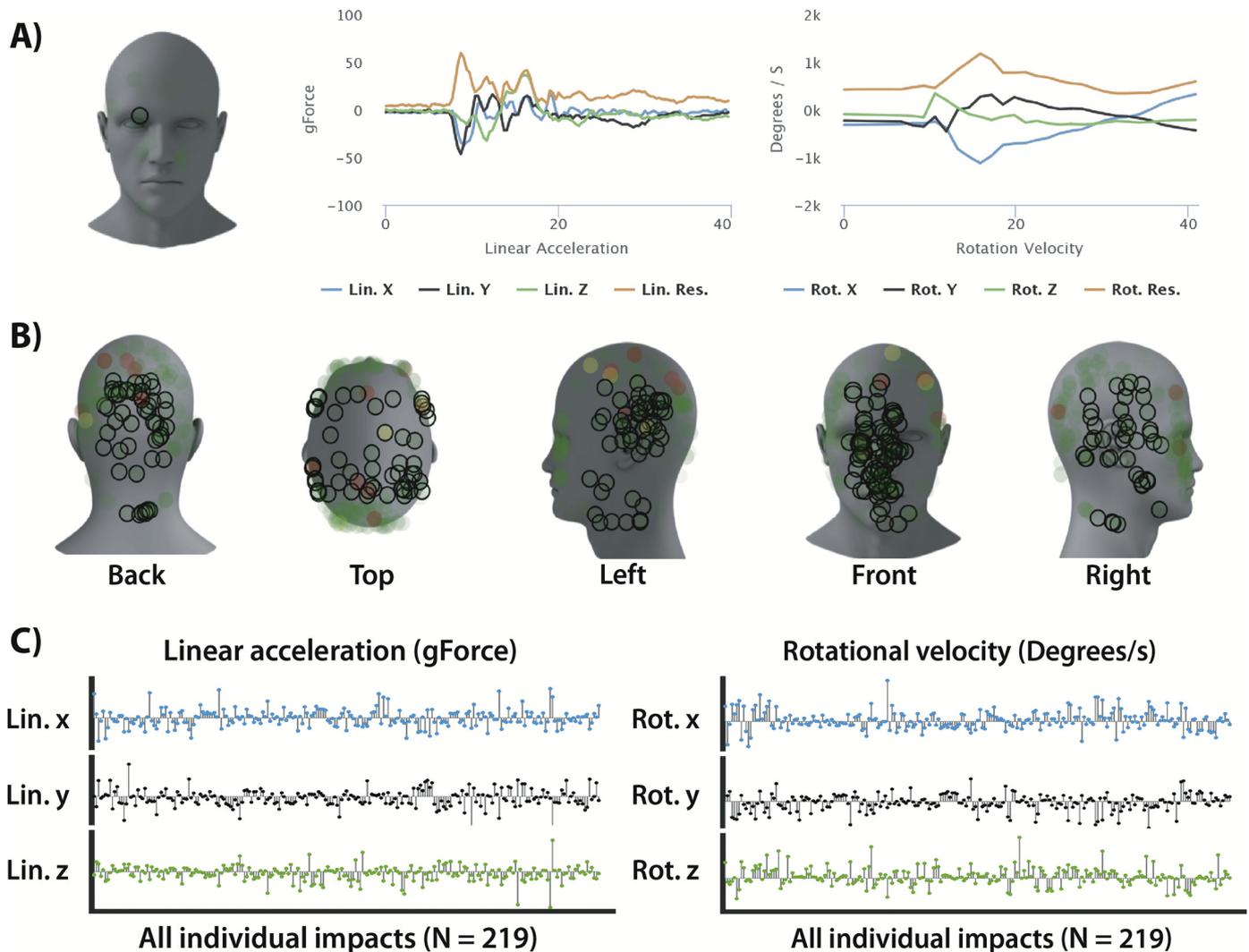
Fig. 2. Sample data from the gForce tracker helmet accelerometer. **(A)** Individual impact location (circle in front) and linear (left) and rotational (right) time-dependent profiles for the x, y and z coordinates. **(B)** Summary of all impacts locations ($N = 219$) sustained by one player between the pre-season (*PRE*) and follow-up (*PTC*) scanning time points. **(C)** Individual x, y and z biomechanical features which make up the resultant peak linear acceleration and rotational velocity. Lin = linear, rot = rotational.

was reconstructed using a linear surround subtraction between the adjacent tag and control volumes of the first echo (TE = 10 ms). Pre-processing steps for the HC and HO data included brain extraction (*BET*), motion correction (FSL *MCFLIRT*; Jenkinson et al. 2002; Mark Jenkinson and Peter Bannister, 2002), co-registration in native space using boundary-based registration (Greve and Fischl 2009), spatial smoothing (8 mm FWHM), band-pass filtering to remove signal drift, and despiking. Then, the ASL data from each block paradigm were converted to physiological units using the single-blood compartment model ((Eq. (1); Wang et al. 2003):

$$CBF = \frac{6000\lambda \cdot \Delta M \cdot R_{1b}}{2\alpha_{inv} \cdot M_0 \cdot (e^{-PLD \cdot R_{1b}} - e^{-(\tau+PLD) \cdot R_{1b}})}\left[\frac{\frac{ml}{100g}}{min}\right]. \tag{1}$$

The following parameters determined using the literature and scanning parameters were used to solve for CBF: blood/tissue water partition coefficient (λ) = 0.9 ml/g (Herscovitch and Raichle 1985), labelling duration (τ) = 1.665 s, and arterial blood longitudinal relaxation rate ($R_{1b} = 1/T_{1b}$) = 1/1.650 s (Zhang et al. 2012). A slice time correction for the differences in PLD due to the two-dimensional EPI readout was also introduced between each axial slices (Alsop et al. 2015). For images acquired during baseline and HO breathing, the

inversion efficiency (α_{inv}) was set to 0.84. During HC, α_{inv} was set to 0.80 to account for the higher blood flow velocity in the feed arteries, in response to the higher arterial CO_2 content (Aslan et al. 2010). The vasoconstrictive effects of HO (Bulte et al. 2007) on CBF were also accounted for on a per-volume basis based on the method proposed in Germuska et al. (2016) and the linear relationship between R_1 and PaO_2 (Ma et al. 2014). Once pre-processed, the HC and HO data were input into the Gauthier calibration (Gauthier et al. 2012) to solve for M, on a voxel per voxel basis.

In addition to the voxelwise M maps, which are used in the next section to derive the $CMRO_2$ timeseries, the CBF_0 and BOLD-CVR maps were derived from the HC data. This is because both CBF_0 and CVR can potentially bias BOLD-based rs-fMRI estimation of FC, by way of the interplay between regional differences in signal- and noise-driven correlations (Chu et al. 2018; Golestani et al. 2016; Liu 2013; Qiu et al. 2017). CBF_0 maps were computed by averaging all baseline volumes while BOLD-CVR maps were calculated by dividing the magnitude change in BOLD signal from the change in end-tidal CO_2 during HC ($BOLD(CVR) = \% \Delta BOLD_{HC}/\Delta P_{ET}CO_2$). To avoid bias in CVR estimates due to regional temporal delays in time to peak (Champagne et al. 2017; Donahue et al. 2016; Duffin et al. 2015; Poublanc et al. 2015), the final 80 s of the block stimulus (120 s) were used to estimate the
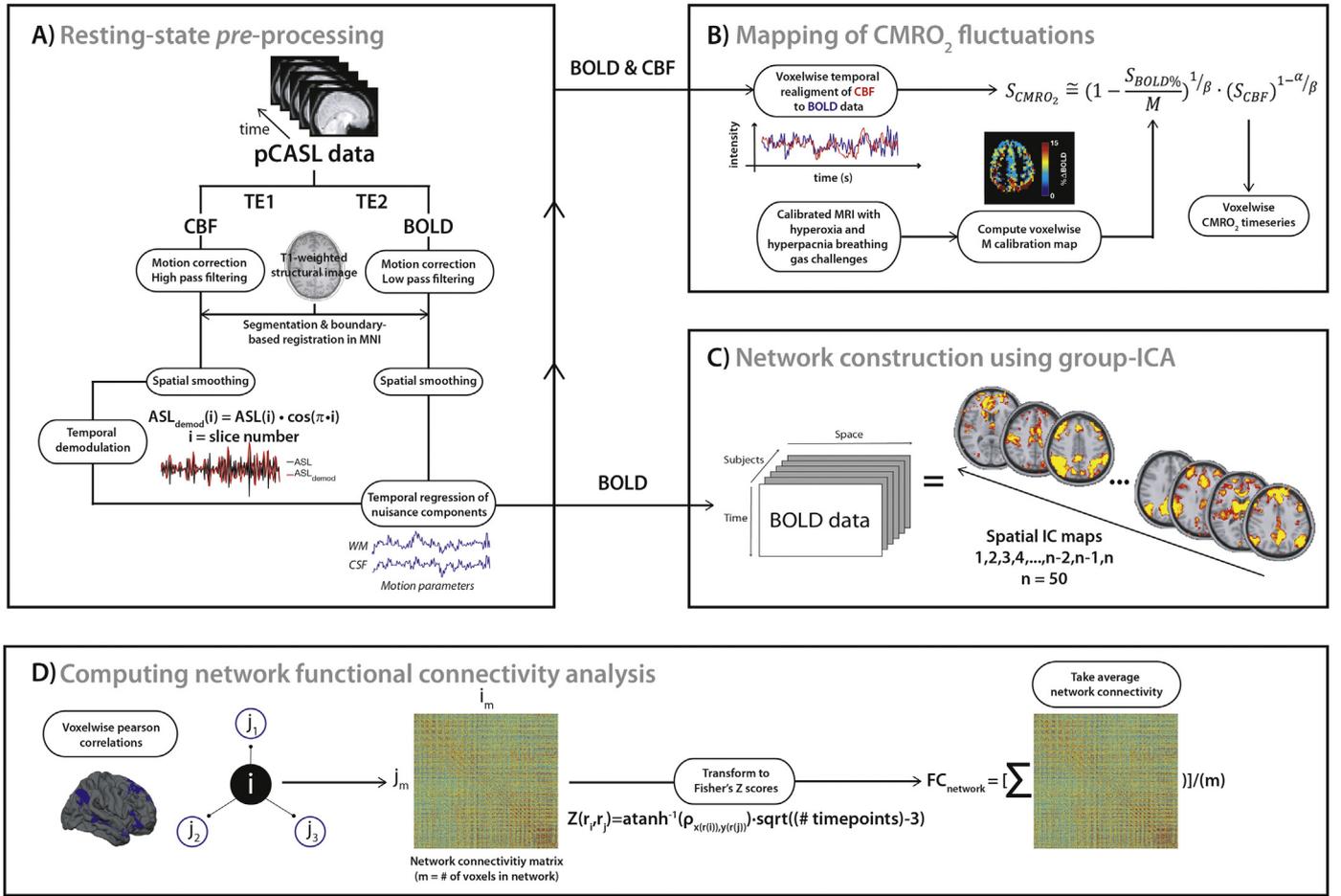
Fig. 3. Schematic of the proposed method for resting-state pre-processing, voxelwise mapping of CMRO$_2$ timeseries and computation of functional connectivity. The modules include the pre-processing of the dual-echo pseudo-continuous (pCASL) data **(A)**, the calibration of the BOLD signal (second echo) using the concurrent perfusion signal (first echo) and the voxelwise M parameter map (determined from quantitative calibrated MRI using hypercapnia and hyperoxia breathing challenges) **(B)**, and the estimation of the network-specific functional connectivity strength **(D)** which was calculated in each subject as the averaged voxelwise connectivity from the regions defined using independent component analysis **(C)**.

relative change in BOLD (%Δ) from baseline.

Coupling between rs-BOLD and -CBF fluctuations is highly variable across the brain (Tak et al. 2014), and over time, especially within major nodes of well-established RS network nodes such as the DMN. To assess the confounding effect of BOLD-CBF coupling on changes in connectivity over time, the coupling coefficient between each signal was computed on a voxel-wise basis. Potential time shifts between the BOLD- and perfusion-based signal were corrected based on cross-correlations (Fig. 3B; Chang and Glover 2009; Frederick et al. 2012; Tong and Frederick, 2010, 2012), and a lag range of −3.5 s to +3.5 s (Fukunaga et al. 2008). Once re-aligned, Pearson correlations between the CBF and BOLD signal were computed at each voxel to measure the degree of concordance between each time series, using a statistical threshold of $P < 0.01$.

2.6. Resting-state calibration and CMRO$_2$ mapping

The M maps were warped non-linearly to 2 mm MNI space using transformation matrices calculated above, to match the spatial resolution of the resting state BOLD and CBF volumes. Then, the BOLD ($S_{BOLD\%}$) and perfusion (S_{CBF}) timeseries, along with the voxelwise M map, were used to derive the CMRO$_2$ (S_{CMRO2}) time course for each voxel (Fig. 3B), using the following equation (Chiarelli et al. 2007; Davis et al. 1998; Wu et al. 2009):

$$S_{CMRO_2} \cong \left(1 - \frac{S_{BOLD\%}}{M}\right)^{1/\beta} \cdot (S_{CBF})^{1-\alpha/\beta}. \tag{2}$$

In Eq. (2), M is replaced by the voxelwise map calculated above, α; which represents the Grubb coefficient modelling the non-linear coupling between flow and venous volume ($CBV/CBV_0 \sim (CBF/CBF_0)^\alpha$), was set to 0.18 (Chen and Pike 2010), and β; which relates the change in dHb concentration to R_2^*, was set to 1.3 (appropriate for field strength of 3.0 T; Boxerman et al. 1995).

2.7. Data analysis

2.7.1. Network construction and calculation of functional connectivity strength

Major resting networks were reconstructed using group spatial Independent Component Analysis (ICA) in FSL's *MELODIC* (Jenkinson et al. 2012). Group-level ICA was repeated at each time point to properly separate neural-related signals from different sources of noise and variability across subjects (Beckmann 2012; Murphy et al. 2013). A total of 50 dimensions were pre-set for the component analysis (Fig. 3C). All resulting components were visually inspected and overlaid onto the well-known functionally-defined brain network atlas from Shirer et al. (2012) for manual interpretation, and identification of the DMN (Griffanti et al. 2017).

Individual-based FC-strength was estimated using the masked components identified from the ICA at each time point (threshold at

$t > 4$). Voxel-based network-wide correlations were computed where each voxel's timecourse, within a network mask, was correlated to all other timeseries. As a result, a $m \times m$ matrix of Pearson correlation coefficients was obtained, where m represents the total number of voxels within the mask (Fig. 3D). The matrix of correlation values was then converted to Fisher Z transforms (Fisher 1915) to stabilize the variance of the distribution in Pearson coefficients. Once transformed, coefficient scores were averaged across the network to reflect the overall FC strength (Fig. 3D). This was repeated for both the BOLD and $CMRO_2$ timeseries in the network of interest (DMN).

2.8. Statistical analysis

The effects of time on network mean CBF_0, BOLD-CVR, BOLD-CBF neurovascular coupling and FC strength were assessed using a two-factor linear mixed model for repeated measures. Time (i.e., overall comparison of PRE vs. PTC vs. POST) was the first factor modeled as a fixed effect, while subject was modeled as a random variable. Due to the confounding effects of baseline end-tidal CO_2 ($P_{ET}CO_2$) on baseline perfusion (Ainslie and Duffin 2009; Battisti-Charbonney et al. 2011), subject-specific mean baseline $P_{ET}CO_2$ was used as a time-varying covariate in the model assessing differences in CBF_0. The BOLD-based analysis of FC strength was corrected for time variations in CBF_0, BOLD-CVR and BOLD-CBF coupling, which were added as covariates in the statistical model. Statistical significance of the confounding variables, set a $P < 0.05$, would suggest that time varying physiological parameters may contribute to changes in DMN connectivity. These factors were not included in the analyses of the $CMRO_2$-based DMN connectivity because the calibration model accounts for regional physiology through the M parameter and the concurrent perfusion measurements (TE_1). The analysis was repeated with and without the adjustment for history of concussion, given the possible long-term effects of sport-related concussion on brain connectivity (Churchill et al. 2017). Statistically significant effects of time for any parameter (set a $P < 0.05$) were followed up with multiple direct pairwise comparisons of the sessions (i.e., PRE vs. PTC, PRE vs. POST, and PTC vs. POST), in order to assess differences between time points.

The relationships between neuroimaging changes from PRE to PTC and impact exposure were assessed using multiple linear regression. The three mean impact kinematics measurements per session were correlated with the magnitude change in network BOLD- and $CMRO_2$-based connectivity between the PRE and PTC time points for the 15 players that returned for imaging at the PTC time point (Fig. 1). Only impacts with a linear acceleration threshold of 25 g and above were considered in the weighting of the impact exposure (Slobounov et al. 2017). All statistical tests were performed in IBM SPSS statistics (version 24.0, SPSS Inc., Chicago, IL, USA).

3. Results

Between the PRE and PTC time points, athletes sustained 6.8 ± 3.0 impacts per session (Table 2), on average. Frequency of head impacts per session ranged from 3.6 ± 2.4 to 13.0 ± 6.8, which were both for TEs, which indicates that exposure is athlete-specific and variability even within a position can be large. Standard deviations for the frequency of impacts per sessions were also large. Peak linear acceleration and rotational velocity for all 15 athletes reached an average of 41.9 ± 4.2 g and 572.9 ± 89.1°/s, respectively (Table 2).

Group ICA at each time point provided robust spatial characteristics of the DMN, which co-localized well with the previous literature (Figs. 4 and 5). Group DMN connectivity was also noticeably more pronounced in the left hemisphere, following thresholding ($t > 4$) of the ICA results (Fig. 4A).

Regional differences in CBF_0 ($P = 0.017$) were observed across time points (Table 3). Pairwise comparisons showed that DMN CBF_0 was significantly decreased one month post-season (POST), when compared

to both the PRE ($P = 0.034$) and PTC ($P = 0.007$) time points. This was true following correction for the effect of $P_{ET}CO_2$, which had no significant effect on CBF_0 ($P = 0.058$). Differences in DMN regional BOLD-CVR were also documented over time ($P = 0.030$), with significant lower CVR measurements at mid-season (PTC; $P = 0.047$) and recovery (POST; $P = 0.018$) time points, compared to PRE-season baseline (Table 3). As opposed to regional CBF_0 and BOLD-CVR, no significant differences in BOLD-CBF neurovascular coupling ($P = 0.907$) were found within the DMN (Table 3). The analysis of regional physiology was repeated with history of concussion as a covariate. There was a significant confounding effect ($P = 0.012$) for concussion history on regional differences in DMN BOLD-CVR ($P = 0.021$ corrected) only. The analyses of DMN CBF_0, and BOLD-CBF coupling were not confounded by differences in concussion history, within the group.

BOLD-based DMN connectivity was significantly increased over time ($P = 0.002$, Fig. 5), with greater group FC strength at the PTC ($P = 0.014$) and POST ($P = 0.0004$) time points, compared to PRE-season baseline. No significant confounding effect on connectivity was observed for regional CBF_0 ($P = 0.205$), BOLD-CVR ($P = 0.162$), BOLD-CBF coupling ($P = 0.453$) or concussion history ($P = 0.661$). $CMRO_2$-based DMN connectivity showed similar significant differences over time ($P = 0.013$, Fig. 5), with increases found between the PRE-PTC ($P = 0.037$) and PRE-POST ($P = 0.026$) time points. Again, concussion history did not confound $CMRO_2$-based differences in connectivity over time ($P = 0.949$).

Summary helmet kinematic features were not correlated with the magnitude of the change in BOLD- or $CMRO_2$-based connectivity between the PRE and PTC time points.

4. Discussion

4.1. Main findings

This study is the first to combine calibrated RS imaging and helmet telemetry to comprehensively examine the underlying changes in network FC following exposure to sub-concussive impacts. The main findings are three-fold: First, significant changes in regional BOLD-CVR and CBF_0 were observed within the DMN, although these differences did not significantly confound changes in BOLD-based DMN connectivity. Second, DMN hyper-connectivity was observed over time and this was consistent for both BOLD- and $CMRO_2$-based FC measurements, following correction for local physiological modulators. Finally, exposure data from the helmet accelerometers was not significantly correlated with changes in DMN connectivity.

4.2. Alterations in network-specific hemodynamic parameters throughout a season of football

Asymptomatic football athletes with no reported SRC during the season exhibited regional changes in CBF_0 within the DMN, with reduced perfusion observed one month after the conclusion of participation in contact activities, confirming that baseline flow may be altered after the season. In Slobounov et al. (2017), higher CBF_0 was found across several regions of the brain after exposure to sub-concussive head impacts. Though we did not find significant differences in perfusion between the PRE and PTC time points, we observed a small increase in CBF_0 for two-thirds of the players within the DMN (data not shown). In addition to fluctuations in CBF_0, the football athletes showed significant regional decreases in BOLD-CVR within the DMN, suggesting changes in the ability of the cerebrovascular vessels to respond to the hypercapnic stimulus. This is similar to previous literature by Svaldi et al. (2015, 2017), who reported decreased fronto-temporal CVR in high-school female soccer players following exposure to sub-concussive head trauma. These changes persisted 4 to 5 months post-season. Changes in BOLD-CVR observed in this cohort mid-season were also persistent one month following the end of the season, confirming

Table 2
Cumulative impact data for the subjects included in the regression analysis between the imaging findings and helmet biometrics.

Subject number	Position	Starting status	Number of sessions recorded	Frequency per session	Peak linear acceleration per session (g)	Peak rotational velocity per session (°/s)
1	DB	starter	20	5.7 ± 5.3	38.1 ± 8.2	515.6 ± 157.8
2	WR	starter	4*	5.3 ± 5.1	43.4 ± 13.8	508.7 ± 174.6
3	LB	back-up	18	3.9 ± 3.8	38.1 ± 14.8	505.6 ± 222.0
4	OL	starter	13	6.5 ± 2.6	37.8 ± 4.6	579.3 ± 115.6
5	TE	starter	14	3.6 ± 2.4	39.7 ± 12.1	441.3 ± 201.2
6	LB	starter	15	9.1 ± 7.6	49.7 ± 8.1	659.1 ± 166.8
7	S	starter	17	5.8 ± 8.1	38.2 ± 10.2	491.8 ± 246.6
8	LB	back-up	13	6.0 ± 4.0	44.1 ± 9.1	731.3 ± 218.2
9	DL	back-up	17	11.5 ± 5.2	44.5 ± 8.2	672.6 ± 105.0
10	TE	starter	14	13.0 ± 6.8	40.3 ± 3.7	497.8 ± 106.8
11	WR	back-up	11	6.8 ± 6.1	48.3 ± 18.6	619.0 ± 157.5
12	DB	back-up	16	3.9 ± 3.2	36.0 ± 7.5	542.4 ± 147.1
13	WR	starter	10*	3.9 ± 3.5	45.2 ± 18.0	718.6 ± 255.9
14	DL	starter	15	11.1 ± 7.7	40.3 ± 6.3	587.9 ± 133.3
15	DB	starter	6*	6.3 ± 3.8	45.3 ± 10.8	522.0 ± 161.1
Mean ± SD	N/A	N/A	13.5 ± 4.2	6.8 ± 3.0	41.9 ± 4.2	572.9 ± 89.1

Values are in mean ± standard deviation. * = Denotes players who had missing accelerometer data due to issues with the impact monitoring system. DB = defensive back, DL = defensive line, LB = linebacker, OL = offensive lineman, S = safety, SD = standard deviation TE = tight-end, WR = wide receiver.

that quantifiable changes in the cerebrovasculature may occur despite athletes being asymptomatic. Although the physiological basis for transient changes in BOLD-CVR remains unknown, recent work by Adams et al. (2018) proposed that changes in vascular reactivity may arise from morphological changes in perivascular density. This however, remains an area of active research. Of note, changes in BOLD-CVR were maintained between the PTC and POST time points, suggesting that the acute and cumulative mechanical loading of head impacts may have a different time course with respect to their effect on cerebral physiology. BOLD-CVR may be more sensitive after acute onset to contact, whereas perfusion-based changes may take longer to develop, hence why significant CBF_0 differences in this cohort were only observed after the season. This observation would also support the discrepancy between Slobounov et al. (2017) and our findings, as they studied perfusion changes after the whole season, and not just the first third (e.g. PTC). Despite changes in CBF_0 and BOLD-CVR, no significant differences in regional coupling were observed, which suggests that although baseline (e.g. CBF_0) and dynamic (e.g. BOLD-CVR) physiological parameters may be altered, the relationship between BOLD- and CBF-based fluctuations was maintained throughout the season.

4.3. Fluctuations in default mode network connectivity during and following the season

In this study, we observed increased DMN connectivity over time. These results were consistent after correcting for the confounding effects of regional hemodynamic measures (e.g. CBF_0, BOLD-CVR, BOLD-CBF coupling), and when using a more direct measurement of neural activity with the calibrated $CMRO_2$ time series. Our findings are in

concordance with previous literature (Abbas et al. 2015a, 2015b; Johnson et al. 2014; Reynolds et al. 2017b), and add robust evidence to the growing body of work suggesting that changes in brain connectivity may result from participation in collision sports, in parallel to changes in cerebrovascular physiology. Clinically, changes in DMN connectivity have also been observed in mild traumatic brain injuries (Zhou et al. 2012), as well as in retired professional athletes with history of concussion (Esopenko et al. 2015), indicating that alterations in brain connectivity may follow both concussive and sub-concussive head trauma. In this study, a specific focus was around studying the DMN given previous evidence for BOLD-based changes in FC. Consistent findings within the DMN across different study groups suggests that certain network structures such as the DMN may be more prone to reorganization following exposure to sub-concussive impacts. The reasons for this susceptibility are currently unknown. However, different factors such as the regio-specificity of the network nodes, and the spatial distribution of strain forces on tissues following different impacts (Elkin et al. 2018) may contribute to these differences.

Confounding vascular factors did not have a significant effect on BOLD connectivity differences across time point. These findings were confirmed with $CMRO_2$-based connectivity, which suggests that changes in FC following exposure to head impacts may be robust and independent of regional changes in brain hemodynamics. Thus, future research should be directed towards examining the underlying mechanisms that lead to hyper-connectivity patterns following head impacts. This may allow identification of potential substrates for compensation at the neuronal level that allows for maintained brain functionality despite imaging changes.
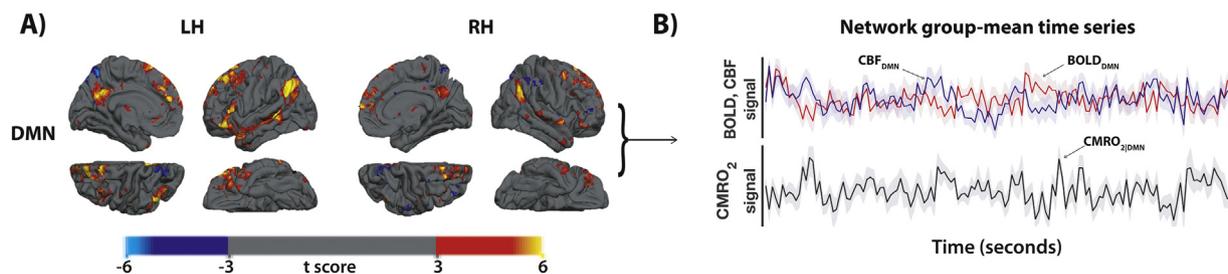
Fig. 4. Results of the group-based independent component analysis (ICA) for network reconstruction in the baseline subjects (PRE). **(A)** The panel shows the independent component network map for the left (LH) and right (RH) hemispheres of the default mode network (DMN), displayed onto the freesurfer template in standard MNI space (2 mm-isotropic). **(B)** The group averaged BOLD (red), CBF (blue) and $CMRO_2$ (black) timeseries (± standard error) for the network. BOLD = blood oxygen level dependent, CBF = cerebral blood flow, $CMRO_2$ = cerebral metabolic rate of oxygen consumption, MNI = Montréal Neurological Institute.
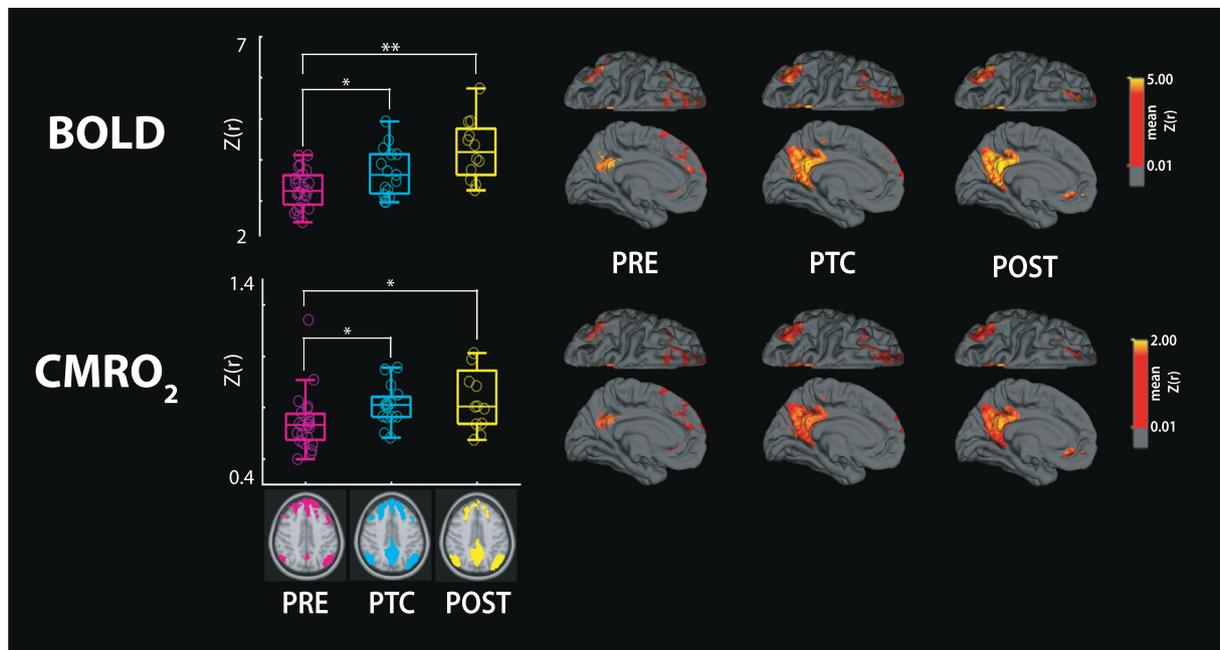
Fig. 5. Boxplot results for changes in connectivity throughout the season. BOLD- (top row) and $CMRO_2$- (bottom row) based connectivity for each time point (x-axis) in the DMN. The color-coded time points PRE (magenta), PTC (cyan) and POST (yellow) show changes in DMN connectivity over time. Group-averaged connectivity maps across time points are also displayed onto the freesurfer template in standard MNI space (2 mm-isotropic). The left medial (bottom row) and superior (top row) views are shown for the DMN. Connectivity values are shown in Fisher Z transforms (Z(r)). *$P < 0.05$, **$P < 0.0005$, BOLD = blood oxygen level dependent, $CMRO_2$ = cerebral metabolic rate of oxygen consumption, DMN = default-mode network, MNI = Montréal Neurological Institute.

Table 3
Statistical results for regional CBF_0, BOLD-CVR, and BOLD-CBF neurovascular coupling over time.

Metric	Mean ± standard deviation			*P*-values
	PRE	PTC	POST	
CBF_0 (ml/min/100 g)[a]	65 ± 7	68 ± 8	62 ± 7	**0.017**^*#^
BOLD-CVR (%ΔBOLD/ $\Delta P_{ET}CO2$)[b]	0.29 ± 0.07	0.26 ± 0.06	0.25 ± 0.05	**0.030**^*^
BOLD-CBF coupling (Z)[b]	2.94 ± 0.66	3.03 ± 0.49	3.02 ± 0.68	0.907

[a] = Statistically compared using a two-factor linear mixed model for repeated measures with end-tidal CO_2 as a time-varying covariate. [b] = Statistically compared using a two-factor linear mixed model for repeated measures. ^ = $P < 0.05$ between PRE and PTC, * = $P < 0.05$ between PRE and POST, # = $P < 0.05$ between PTC and POST. BOLD = blood oxygen level dependent, DMN = default-mode network, CBF_0 = resting cerebral blood flow, CVR = cerebrovascular reactivity, PRE = baseline time point, PTC = *post*-training camp time point, POST = post-season time point.

4.4. Poor relationship between changes in network connectivity and impact biomechanics

Helmet accelerometer data reported in this study is the first to provide evidence for the daily exposure of Canadian collegiate football players at various in positions. Compared to previous literature on American collegiate athletes (Crisco et al., 2010, b; Mihalik et al. 2007), mean linear accelerations reported in this study were higher, on average, likely due to the higher force threshold used for the analysis (i.e. 25 g vs. 10 g (Mihalik et al., 2007) or 14.4 g (Crisco et al., 2010, b)), which was chosen because of the previous methodological design in Slobounov et al. (2017). In terms of frequency of impacts per athlete exposure exceeding 25 g, players studied in this cohort sustained on average 6.8 ± 3.0 impacts per session, compared to 4.3 ± 2.4 impacts per session in Slobounov et al., (2017; extrapolated from Table 1). The difference between these frequencies is likely related to variability in

position studied, the differences between the helmet tracking system (gForce tracker vs. BodiTrak system in Slobounov et al. (2017)) and possibly, differences between Canadian and American football. Some of those differences include a larger playing field in Canadian football, along with the ability to have various motions for skilled athletes prior to the snap. This may allow players to achieve maximum running speed more frequently. Other differences include a full yard separating the offensive and defensive linemen, as well as an additional player on the field, for a total of 12 athletes per team, as opposed to 11 in American football. Further research on the effects of rule changes in Canadian football, as well as the standardization of equipment with respect to impact monitoring system will help further advance this field of research.

In order to investigate the relationship between changes in network connectivity and exposure to head impacts, we correlated common daily exposure metrics with the magnitude of change in FC between the PRE and PTC time points. No significant relationship was observed between the changes in DMN FC measurements and any of the helmet biometric measures. The lack of relationship with neuroimaging findings suggests that helmet-based sensors may be limited in predicting changes in the brain, following exposure to impacts, possibly due to limitations in the accuracy and reliability of the data acquired (Cummiskey et al. 2017), or poor correlations between trauma and changes in connectivity. Furthermore, it is worth acknowledging that despite the validation provided by (Campbell et al. 2016), rotational measurements provided by helmet-based technologies like the GFT can be biased by possible relative motion between the head and the helmet, which would further limit the accuracy of rotational measurements reported in this study. Lastly, no additional correction algorithms were applied to the raw GFT data, in order to transform linear and angular measurements from the helmet shell to the center of mass of the head. This may also be a possible source of error limiting the potential for the kinematic measures to predict changes in the brain, as such corrections may prevent overestimation of the peak linear accelerations. Consensus for proper calibration of the quantitative measures recorded using the helmet-mounted sensors should be considered in future research

designs.

4.5. Limitations

Some factors and assumptions may limit the interpretation of the results reported in this study. As with other neuroimaging studies of collision sport athletes, our sample size was limited and not constant across different sessions, due to SRCs and season-ending injuries. Though we attempted to limit this effect using a linear mixed statistical model, this may have influenced our results given that only 12 athletes were scanned at that POST time point, one month after the season. In this design, we used a global mean connectivity measure as an overall index for network connectivity. However, such a measure does not provide an accurate picture of the node to node variations in connectivity, which limits our understanding of the potential seed-specific alterations within each network. Our design also did not include a control group of non-contact sport athletes, which limits our characterization of the variability in the data independent of the effect of head impacts. The lack of control group also limits our ability to control for the effect of exercise and other physiological factors like fitness that may contribute to changes in cerebral physiology (Mairbäurl 2013). However, the possible effect of exercise on baseline physiology is unlikely to affect the changes in connectivity reported here, as these were independent of the changes in brain hemodynamics across the time points.

In addition to limitations within the study design, other physiological parameters relative to RS imaging could be accounted for in future work. For instance, recent work by Chang and Glover (2010) and Deco et al. (2009) has proposed the introduction of temporal delay corrections across regions, which may improve FC measurements within networks. Other methodological approaches such as dynamic connectivity analyses (Hutchison et al. 2013; Preti et al. 2017) may also help account for temporal fluctuations in the brain across different connectivity states, and inherently improve FC measurements. As well, in this calibrated RS study, the Grubb coefficient (α), which relates changes in flow and CBV, was assumed to remain constant ($\alpha = 0.18$) along the resting-state time course. However, it is possible that this value fluctuates over time and that a better model for deriving $CMRO_2$ timecourse includes varying estimates of α. Additionally, because RS-BOLD fluctuations are minimal, dividing the BOLD signal by M in Eq. (2) biases the resultant $CMRO_2$ timecourse towards the ASL signal.

Despite these limitations, this method is the first to delve into the physiology of RS connectivity analyses following head impacts. Limitations such as the ones highlighted above will require additional research as the field of calibrated MRI continues to expand our understanding of the complex physiology underlying the BOLD signal.

5. Conclusion

The purpose of this study was to investigate the effects of sub-concussive head impacts on brain connectivity, while controlling for the possible confounding effects of key vascular hemodynamic factors such as CBF_0, BOLD-CVR and BOLD-CBF coupling, that contribute to RS-FC measurements. Alterations in CBF_0 and BOLD-CVR throughout the season suggests that changes in neurophysiological markers may occur on a different timeline following head impacts. This is a key finding moving forward as it highlights that different pathological mechanisms within the cerebral vasculature may be responsible for driving changes in physiology that occur at different rates following exposure to sub-concussive head impacts. Alterations in BOLD- and $CMRO_2$-based connectivity were observed in addition to changes in regional network perfusion and vascular reactivity. Despite finding decreases in CBF_0 and BOLD-CVR within the networks, changes in cerebral physiology did not significantly confound the increases in DMN network connectivity throughout the season. These findings emphasize that exposure to head impacts may alter specific connectivity

patterns within the brain, in parallel to changes in cerebrovascular physiology. Lastly, our results provide more evidence on the limited predictive capacity of simple kinematic features to determine differences in neuroimaging findings following head impacts, across different football athletes. Altogether, these findings create a strong paradigm for future studies to examine the underlying neural and vascular mechanisms associated with increases in network connectivity following repeated exposure to head impacts. Novel tools such as calibrated MRI may allow us to better understand how changes in brain network organization and vascular physiology related to head impacts may be reduced, as we strive to make sports safer.

References

Abbas, K., Shenk, T.E., Poole, V.N., Breedlove, E.L., Leverenz, L.J., Nauman, E.A., Talavage, T.M., Robinson, M.E., 2015a. Alteration of default mode network in high school football athletes due to repetitive subconcussive mild traumatic brain injury: a resting-state functional magnetic resonance imaging study. Brain Connect. 5, 91–101. https://doi.org/10.1089/brain.2014.0279.

Abbas, K., Shenk, T.E., Poole, V.N., Robinson, M.E., Leverenz, L.J., Nauman, E.A., Talavage, T.M., 2015b. Effects of repetitive sub-concussive brain injury on the functional connectivity of default mode network in high school football athletes. Dev. Neuropsychol. 40, 51–56. https://doi.org/10.1080/87565641.2014.990455.

Adams, C.R., Bazzigaluppi, P., Beckett, T.L., BBishay, J., Steinman, J., Hirschler, L., Warnking, J.M., Barkier, E.L., McLaurin, J., Sled, J.G., Stefanovic, B., 2018. Chronic Neurovascular Dysfunction in a Mouse Model of Repeated Mild Traumatic Brain Injury (Conference Abstract). ISMRM.

Ainslie, P.N., Duffin, J., 2009. Integration of cerebrovascular CO2 reactivity and che-moreflex control of breathing: mechanisms of regulation, measurement, and interpretation. Am. J. Phys. Regul. Integr. Comp. Phys. 296. https://doi.org/10.1152/ajpregu.91008.2008.

Alsop, D.C., Detre, J.A., Golay, X., Gunther, M., Hendrikse, J., Hernandez-Garcia, L., Lu, H., Macintosh, B.J., Parkes, L.M., Smits, M., Van Osch, M.J.P., Wang, D.J.J., Wong, E.C., Zaharchuk, G., 2015. Recommended implementation of arterial spin-labeled perfusion mri for clinical applications: a consensus of the ISMRM perfusion study group and the European consortium for ASL in dementia. Magn. Reson. Med. 73, 102–116. https://doi.org/10.1002/mrm.25197.

Andersson, J.L.R., Jenkinson, M., Smith, S., 2007. Non-linear Registration Aka Spatial Normalisation FMRIB Technial Report TR07JA2. (In Pract. 22).

Aslan, S., Xu, F., Wang, P.L., Uh, J., Yezhuvath, U.S., Van Osch, M., Lu, H., 2010. Estimation of labeling efficiency in pseudocontinuous arterial spin labeling. Magn.

Reson. Med. 63, 765–771. https://doi.org/10.1002/mrm.22245.

Battisti-Charbonney, A., Fisher, J., Duffin, J., 2011. The cerebrovascular response to carbon dioxide in humans. J. Physiol. 589, 3039–3048. https://doi.org/10.1113/jphysiol.2011.206052.

Beckmann, C.F., 2012. Modelling with independent components. Neuroimage. https://doi.org/10.1016/j.neuroimage.2012.02.020.

Biswal, B.B., Kannurpatti, S.S., Rypma, B., 2007. Hemodynamic scaling of fMRI-BOLD signal: validation of low-frequency spectral amplitude as a scalability factor. Magn. Reson. Imaging 25, 1358–1369. https://doi.org/10.1016/j.mri.2007.03.022.

Boxerman, J.L., Hamberg, L.M., Rosen, B.R., Weisskoff, R.M., 1995. Mr contrast due to intravascular magnetic susceptibility perturbations. Magn. Reson. Med. 34, 555–566. https://doi.org/10.1002/mrm.1910340412.

Broglio, S.P., Eckner, J.T., Martini, D., Sosnoff, J.J., Kutcher, J.S., Randolph, C., 2011. Cumulative head impact burden in high school football. J. Neurotrauma 28, 2069–2078. https://doi.org/10.1089/neu.2011.1825.

Broglio, S.P., Surma, T., Ashton-Miller, J.A., 2012. High school and collegiate football athlete concussions: a biomechanical review. Ann. Biomed. Eng. 40, 37–46. https://doi.org/10.1007/s10439-011-0396-0.

Brosch, J.R., Talavage, T.M., Ulmer, J.L., Nyenhuis, J.A., 2002. Simulation of human respiration in fMRI with a mechanical model. IEEE Trans. Biomed. Eng. https://doi.org/10.1109/TBME.2002.1010854.

Bulte, D.P., Chiarelli, P. a, Wise, R.G., Jezzard, P., 2007. Cerebral perfusion response to hyperoxia. J. Cereb. Blood Flow Metab. 27, 69–75. https://doi.org/10.1038/sj.jcbfm.9600319.

Campbell, K.R., Warnica, M.J., Levine, I.C., Brooks, J.S., Laing, A.C., Burkhart, T.A., Dickey, J.P., 2016. Laboratory evaluation of the gForce tracker™, a head impact kinematic measuring device for use in football helmets. Ann. Biomed. Eng. 44, 1246–1256. https://doi.org/10.1007/s10439-015-1391-7.

Carusone, L.M., Srinivasan, J., Gitelman, D.R., Mesulam, M.M., Parrish, T.B., 2002. Hemodynamic response changes in cerebrovascular disease: implications for functional MR imaging. AJNR Am. J. Neuroradiol. 23, 1222–1228.

Champagne, A.A., Bhogal, A.A., Coverdale, N.S., Mark, C.I., Cook, D.J., 2017. A novel perspective to calibrate temporal delays in cerebrovascular reactivity using hypercapnic and hyperoxic respiratory challenges. Neuroimage 11.

Chang, C., Glover, G.H., 2009. Effects of model-based physiological noise correction on default mode network anti-correlations and correlations. Neuroimage 47, 1448–1459. https://doi.org/10.1016/j.neuroimage.2009.05.012.

Chang, C., Glover, G.H., 2010. Time-frequency dynamics of resting-state brain connectivity measured with fMRI. Neuroimage 50, 81–98. https://doi.org/10.1016/j.neuroimage.2009.12.011.

Chen, J.J., Pike, G.B., 2010. Global cerebral oxidative metabolism during hypercapnia and hypocapnia in humans: implications for BOLD fMRI. J. Cereb. Blood Flow Metab. 30, 1094–1099. https://doi.org/10.1038/jcbfm.2010.42.

Chiarelli, P.A., Bulte, D.P., Piechnik, S., Jezzard, P., 2007. Sources of systematic bias in hypercapnia-calibrated functional MRI estimation of oxygen metabolism. Neuroimage 34, 35–43. https://doi.org/10.1016/j.neuroimage.2006.08.033.

Chu, P.P.W., Golestani, A.M., Kwinta, J.B., Khatamian, Y.B., Chen, J.J., 2018. Characterizing the modulation of resting-state fMRI metrics by baseline physiology. Neuroimage. https://doi.org/10.1016/j.neuroimage.2018.02.004.

Chuang, K.H., van Gelderen, P., Merkle, H., Bodurka, J., Ikonomidou, V.N., Koretsky, A.P., Duyn, J.H., Talagala, S.L., 2008. Mapping resting-state functional connectivity using perfusion MRI. Neuroimage 40, 1595–1605. https://doi.org/10.1016/j.neuroimage.2008.01.006.

Churchill, N., Hutchison, M.G., Leung, G., Graham, S., Schweizer, T.A., 2017. Changes in functional connectivity of the brain associated with a history of sport concussion: a preliminary investigation. Brain Inj. 31, 39–48. https://doi.org/10.1080/02699052.2016.1221135.

Cordes, D., Haughton, V.M., Arfanakis, K., Wendt, G.J., Turski, P.A., Moritz, C.H., Quigley, M.A., Meyerand, M.E., 2000. Mapping functionally related regions of brain with functional connectivity MR imaging. Am. J. Neuroradiol. 21, 1636–1644. https://doi.org/10.1016/j.amepre.2011.10.016.

Cox, R.W., 1996. AFNI: software for analysis and visualization of functional magnetic resonance neuroimages. Comput. Biomed. Res. https://doi.org/10.1006/cbmr.1996.0014.

Crisco, J.J., Fiore, R., Beckwith, J.G., Chu, J.J., Brolinson, G.P., Duma, S., McAllister, T.W., Duhaime, A.C., Greenwald, R.M., 2010. Frequency and location of head impact exposures in individual collegiate football players. J. Athl. Train. 45, 549–559. https://doi.org/10.4085/1062-6050-45.6.549.

Crisco, J.J., Wilcox, B.J., Machan, J.T., McAllister, T.W., Duhaime, A.C., Duma, S.M., Rowson, S., Beckwith, J.G., Chu, J.J., Greenwald, R.M., 2012. Magnitude of head impact exposures in individual collegiate football players. J. Appl. Biomech. 28, 174–183. https://doi.org/10.4085/1062-6050-45.6.549.

Cummiskey, B., Schiffmiller, D., Talavage, T.M., Leverenz, L., Meyer, J.J., Adams, D., Nauman, E.A., 2017. Reliability and accuracy of helmet-mounted and head-mounted devices used to measure head accelerations. Proc. Inst. Mech. Eng. Part P J. Sport. Eng. Technol. https://doi.org/10.1177/1754337116658395.

Dai, W., Garcia, D., De Bazelaire, C., Alsop, D.C., 2008. Continuous flow-driven inversion for arterial spin labeling using pulsed radio frequency and gradient fields. Magn. Reson. Med. 60, 1488–1497. https://doi.org/10.1002/mrm.21790.

Davis, T.L., Kwong, K.K., Weisskoff, R.M., Rosen, B.R., 1998. Calibrated functional MRI: mapping the dynamics of oxidative metabolism. Proc. Natl. Acad. Sci. U. S. A. 95, 1834–1839. https://doi.org/10.1073/pnas.95.4.1834.

Deco, G., Jirsa, V., McIntosh, A.R., Sporns, O., Kotter, R., 2009. Key role of coupling, delay, and noise in resting brain fluctuations. Proc. Natl. Acad. Sci. 106, 10302–10307. https://doi.org/10.1073/pnas.0901831106.

Donahue, M.J., Strother, M.K., Lindsey, K.P., Hocke, L.M., Tong, Y., deB Frederick, B., 2016. Time delay processing of hypercapnic fMRI allows quantitative parameterization of cerebrovascular reactivity and blood flow delays. J. Cereb. Blood Flow Metab. 36, 1767–1779. https://doi.org/10.1177/0271678X15608643.

Duffin, J., Sobczyk, O., Crawley, A.P., Poublanc, J., Mikulis, D.J., Fisher, J.A., 2015. The

dynamics of cerebrovascular reactivity shown with transfer function analysis. Neuroimage 114, 207–216. https://doi.org/10.1016/j.neuroimage.2015.04.029.

Elkin, B.S., Gabler, L.F., Panzer, M.B., Siegmund, G.P., 2018. Brain tissue strains vary with head impact location: a possible explanation for increased concussion risk in struck versus striking football players. Clin. Biomech. 1–9. https://doi.org/10.1016/j.clinbiomech.2018.03.021.

Esopenko, C., Sheldon, S., McIntosh, A.R., Strother, S., Levine, B., 2015. Intrinsic functional brain connectivity in retired professional hockey players. J. Head Trauma Rehabil. 30 (3), E99–E100. https://doi.org/10.1097/HTR.0000000000000150.

Findler, P., 2015. Should kids play (American) football? J. Philos. Sport 42, 443–462. https://doi.org/10.1080/00948705.2015.1079132.

Finn, E.S., Shen, X., Scheinost, D., Rosenberg, M.D., Huang, J., Chun, M.M., Papademetris, X., Constable, R.T., 2015. Functional connectome fingerprinting: identifying individuals using patterns of brain connectivity. Nat. Neurosci. 18, 1664–1671. https://doi.org/10.1038/nn.4135.

Fisher, R.A., 1915. Frequency distribution of the values of the correlation coefficient in samples from an indefinitely large population. Biometrika 10, 507. https://doi.org/10.2307/2331838.

Fox, M.D., Snyder, A.Z., Vincent, J.L., Corbetta, M., Van Essen, D.C., Raichle, M.E., 2005. The Human brain is intrinsically organized into dynamic, anticorrelated functional the human brain is intrinsically organized into dynamic, anticorrelated functional networks. Source Proc. Natl. Acad. Sci. U. S. A. 102, 9673–9678.

Frederick, B. deB, Nickerson, L.D., Tong, Y., 2012. Physiological denoising of BOLD fMRI data using Regressor interpolation at progressive time delays (RIPTiDe) processing of concurrent fMRI and near-infrared spectroscopy (NIRS). Neuroimage 60, 1913–1923. https://doi.org/10.1016/j.neuroimage.2012.01.140.

Fukunaga, M., Horovitz, S.G., De Zwart, J.A., Van Gelderen, P., Balkin, T.J., Braun, A.R., Duyn, J.H., 2008. Metabolic origin of BOLD signal fluctuations in the absence of stimuli. J. Cereb. Blood Flow Metab. 28, 1377–1387. https://doi.org/10.1038/jcbfm.2008.25.

Gauthier, C.J., Desjardins-Crépeau, L., Madjar, C., Bherer, L., Hoge, R.D., 2012. Absolute quantification of resting oxygen metabolism and metabolic reactivity during functional activation using QUO2 MRI. Neuroimage 63, 1353–1363. https://doi.org/10.1016/j.neuroimage.2012.07.065.

Germuska, M., Merola, A., Murphy, K., Babic, A., Richmond, L., Khot, S., Hall, J.E., Wise, R.G., 2016. A forward modelling approach for the estimation of oxygen extraction fraction by calibrated fMRI. Neuroimage 139, 313–323. https://doi.org/10.1016/j.neuroimage.2016.06.004.

Golestani, A.M., Kwinta, J.B., Strother, S.C., Khatamian, Y.B., Chen, J.J., 2016. The association between cerebrovascular reactivity and resting-state fMRI functional connectivity in healthy adults: the influence of basal carbon dioxide. Neuroimage 132, 301–313. https://doi.org/10.1016/j.neuroimage.2016.02.051.

Greicius, M.D., Krasnow, B., Reiss, A.L., Menon, V., 2003. Functional connectivity in the resting brain: a network analysis of the default mode hypothesis. Proc. Natl. Acad. Sci. U. S. A. 100, 253–258. https://doi.org/10.1073/pnas.0135058100.

Greicius, M.D., Supekar, K., Menon, V., Dougherty, R.F., 2009. Resting-state functional connectivity reflects structural connectivity in the default mode network. Cereb. Cortex 19, 72–78. https://doi.org/10.1093/cercor/bhn059.

Greve, D.N., Fischl, B., 2009. Accurate and robust brain image alignment using boundary-based registration. Neuroimage 48, 63–72. https://doi.org/10.1016/j.neuroimage.2009.06.060.

Griffanti, L., Douaud, G., Bijsterbosch, J., Evangelisti, S., Alfaro-Almagro, F., Glasser, M.F., Duff, E.P., Fitzgibbon, S., Westphal, R., Carone, D., Beckmann, C.F., Smith, S.M., 2017. Hand classification of fMRI ICA noise components. Neuroimage 154, 188–205. https://doi.org/10.1016/j.neuroimage.2016.12.036.

Herscovitch, P., Raichle, M.E., 1985. What is the correct value for the brain–blood partition coefficient for water? J. Cereb. Blood Flow Metab. 5, 65–69. https://doi.org/10.1038/jcbfm.1985.9.

Hoge, R., Atkinson, J., Gill, B., Crelier, G., Marrett, S., 1999. Investigation of BOLD signal dependence on cerebral blood flow and oxygen consumption. Magn. Reson. Med. 863, 849–863.

Hutchison, R.M., Womelsdorf, T., Allen, E.A., Bandettini, P.A., Calhoun, V.D., Corbetta, M., Della Penna, S., Duyn, J.H., Glover, G.H., Gonzalez-Castillo, J., Handwerker, D.A., Keilholz, S., Kiviniemi, V., Leopold, D.A., de Pasquale, F., Sporns, O., Walter, M., Chang, C., 2013. Dynamic functional connectivity: promise, issues, and interpretations. Neuroimage 80, 360–378. https://doi.org/10.1016/j.neuroimage.2013.05.079.

Jenkinson, Mark, Bannister, Peter, 2002. Improved Methods for the Registration and Motion Correction of Brain Images. vol. 841. pp. 825–841.

Jenkinson, M., Bannister, P., Brady, M., Smith, S., 2002. Improved optimization for the robust and accurate linear registration and motion correction of brain images. Neuroimage 17, 825–841. https://doi.org/10.1016/S1053-8119(02)91132-8.

Jenkinson, M., Beckmann, C.F., Behrens, T.E.J., Woolrich, M.W., Smith, S.M., 2012. Fsl. Neuroimage 62, 782–790. https://doi.org/10.1016/j.neuroimage.2011.09.015.

Jo, H.J., Saad, Z.S., Simmons, W.K., Milbury, L.A., Cox, R.W., 2010. Mapping sources of correlation in resting state FMRI, with artifact detection and removal. Neuroimage 52, 571–582. https://doi.org/10.1016/j.neuroimage.2010.04.246.

Johnson, B., Neuberger, T., Gay, M., Hallett, M., Slobounov, S., 2014. Effects of subconcussive head trauma on the default mode network of the brain. J. Neurotrauma 31, 1907–1913. https://doi.org/10.1089/neu.2014.3415.

Kannurpatti, S.S., Biswal, B.B., 2008. Detection and scaling of task-induced fMRI-BOLD response using resting state fluctuations. Neuroimage 40, 1567–1574. https://doi.org/10.1016/j.neuroimage.2007.09.040.

Kannurpatti, S.S., Motes, M.A., Rypma, B., Biswal, B.B., 2010. Neural and vascular variability and the fMRI-BOLD response in normal aging. Magn. Reson. Imaging 28, 466–476. https://doi.org/10.1016/j.mri.2009.12.007.

Kerr, Z.Y., Hayden, R., Dompier, T.P., Cohen, R., 2015. Association of equipment worn and concussion injury rates in national collegiate athletic association football practices. Am. J. Sports Med. 43, 1134–1141. https://doi.org/10.1177/0363546515570622.

Li, Z., Zhu, Y., Childress, A.R., Detre, J.A., Wang, Z., 2012. Relations between BOLD fMRI-derived resting brain activity and cerebral blood flow. PLoS ONE 7. https://doi.org/10.1371/journal.pone.0044556.

Li, M., Chen, H., Wang, J., Liu, F., Long, Z., Wang, Y., Iturria-Medina, Y., Zhang, J., Yu, C., Chen, H., 2014. Handedness- and hemisphere-related differences in small-world brain networks: a diffusion tensor imaging tractography study. Brain Connect. 4, 1–35. https://doi.org/10.1089/brain.2013.0211.

Liang, X., Zou, Q., He, Y., Yang, Y., 2013. Coupling of functional connectivity and regional cerebral blood flow reveals a physiological basis for network hubs of the human brain. Proc. Natl. Acad. Sci. 110, 1929–1934. https://doi.org/10.1073/pnas.1214900110.

Liu, T.T., 2013. Neurovascular factors in resting-state functional MRI. Neuroimage 80, 339–348. https://doi.org/10.1016/j.neuroimage.2013.04.071.

Ma, Y., Berman, A.J.L., Pike, G.B., 2014. The effect of dissolved oxygen on relaxation rates of blood plasma. In: Proceedings 22nd Scientific Meeting. International Society for Magnetic Resonance in Medicine, pp. 3099.

Mairbäurl, H., 2013. Red blood cells in sports: effects of exercise and training on oxygen supply by red blood cells. Front. Physiol. https://doi.org/10.3389/fphys.2013.00332.

Mandell, D.M., Han, J.S., Poublanc, J., Crawley, A.P., Stainsby, J.A., Fisher, J.A., Mikulis, D.J., 2008. Mapping cerebrovascular reactivity using blood oxygen level-dependent MRI in patients with arterial steno-occlusive disease: comparison with arterial spin labeling MRI. Stroke 39, 2021–2028. https://doi.org/10.1161/STROKEAHA.107.506709.

Martini, D., Eckner, J., Kutcher, J., Broglio, S.P., 2013. Subconcussive head impact biomechanics: comparing differing offensive schemes. Med. Sci. Sports Exerc. 45, 755–761. https://doi.org/10.1249/MSS.0b013e3182798758.

Mccrea, M., Guskiewicz, K.M., Marshall, S.W., Barr, W., Randolph, C., Cantu, R.C., Onate, J. a, Kelly, J.P., Page, P., 2003. Acute effects and recovery time following concussion in collegiate football players. J. Am. Med. Assoc. 290, 2556–2563.

McCrory, P., Meeuwisse, W.H., Aubry, M., Cantu, R.C., Dvorák, J., Echemendia, R.J., Engebretsen, L., Johnston, K.M., Kutcher, J.S., Raftery, M., Sills, A., Benson, B.W., Davis, G.a., Ellenbogen, R., Guskiewicz, K.M., Herring, S.a., Iverson, G.L., Jordan, B.D., Kissick, J., McCrea, M., McIntosh, A.S., Maddocks, D.L., Makdissi, M., Purcell, L., Putukian, M., Schneider, K., Tator, C.H., Turner, M., 2013. Consensus statement on concussion in sport-the 4th international conference on concussion in sport held in Zurich, November 2012. PM R 5, 255–279. https://doi.org/10.1016/j.pmrj.2013.02.012.

Mihalik, J.P., Bell, D.R., Marshall, S.W., Guskiewicz, K.M., 2007. Measurement of head impacts in collegiate football players: an investigation of positional and event-type differences. Neurosurgery 61, 1229–1235. discussion 1235. https://doi.org/10.1227/01.neu.0000306101.83882.c8.

Montenigro, P.H., Alosco, M.L., Martin, B., Daneshvar, D.H., Mez, J., Chaisson, C., Nowinski, C.J., Au, R., McKee, A.C., Cantu, R.C., McClean, M.D., Stern, R.A., Tripodis, Y., 2016. Cumulative head impact exposure predicts later-life depression, apathy, executive dysfunction, and cognitive impairment in former high school and college football players. J. Neurotrauma 0–55. https://doi.org/10.1089/neu.2016.4413.

Murphy, K., Birn, R.M., Bandettini, P.A., 2013. Resting-state fMRI confounds and cleanup. Neuroimage 80, 349–359. https://doi.org/10.1016/j.neuroimage.2013.04.001.

Nasrallah, F.A., Lee, E.L.Q., Chuang, K.H., 2012. Optimization of flow-sensitive alternating inversion recovery (FAIR) for perfusion functional MRI of rodent brain. NMR Biomed. 25, 1209–1216. https://doi.org/10.1002/nbm.2790.

Nelson, L.D., Janecek, J.K., McCrea, M.A., 2013. Acute clinical recovery from sport-related concussion. Neuropsychol. Rev. https://doi.org/10.1007/s11065-013-9240-7.

Ogawa, S., Lee, T.M., Kay, A.R., Tank, D.W., 1990. Brain magnetic resonance imaging with contrast dependent on blood oxygenation. Proc. Natl. Acad. Sci. U. S. A. 87, 9868–9872. https://doi.org/10.1073/pnas.87.24.9868.

Omalu, B., 2015. Don ' T Let Kids Play Football. New York Times. pp. 21–23.

Para, A.E., Sam, K., Poublanc, J., Fisher, J.A., Crawley, A.P., Mikulis, D.J., 2017. Invalidation of fMRI experiments secondary to neurovascular uncoupling in patients with cerebrovascular disease. J. Magn. Reson. Imaging. https://doi.org/10.1002/jmri.25639.

Poublanc, J., Crawley, A.P., Sobczyk, O., Montandon, G., Sam, K., Mandell, D.M., Dufort, P., Venkatraghavan, L., Duffin, J., Mikulis, D.J., Fisher, J. a, 2015. Measuring cerebrovascular reactivity: the dynamic response to a step hypercapnic stimulus. J. Cereb. Blood Flow Metab. 1–11. https://doi.org/10.1038/jcbfm.2015.114.

Preti, M.G., Bolton, T.A., Van De Ville, D., 2017. The dynamic functional connectome: state-of-the-art and perspectives. Neuroimage 160, 41–54. https://doi.org/10.1016/j.neuroimage.2016.12.061.

Qiu, M., Scheinost, D., Ramani, R., Constable, R.T., 2017. Multi-modal analysis of functional connectivity and cerebral blood flow reveals shared and unique effects of propofol in large-scale brain networks. Neuroimage 148, 130–140. https://doi.org/10.1016/j.neuroimage.2016.12.080.

Reynolds, B.B., Patrie, J., Henry, E.J., Goodkin, H.P., Broshek, D.K., Wintermark, M., Druzgal, T.J., 2017a. Comparative analysis of head impact in contact and collision sports. J. Neurotrauma 34, 38–49. https://doi.org/10.1089/neu.2015.4308.

Reynolds, B.B., Stanton, A.N., Soldozy, S., Goodkin, H.P., Wintermark, M., Druzgal, T.J., 2017b. Investigating the effects of subconcussion on functional connectivity using mass-univariate and multivariate approaches. Brain Imaging Behav. 1–14. https://doi.org/10.1007/s11682-017-9790-z.

Sanders, B., 2016. Barry Sanders: should you Let your Kids Play Football? [WWW Document]. USA Today. https://www.usatoday.com/story/opinion/2016/01/24/barry-sanders-let-your-kids-play-football-risks-brain-injury-concussion/79265468/, Accessed date: 26 May 2018.

Schmidt, J.D., Guskiewicz, K.M., Mihalik, J.P., Blackburn, J.T., Siegmund, G.P., Marshall, S.W., 2016. Head impact magnitude in American high school football. Pediatrics 138, e20154231. https://doi.org/10.1542/peds.2015-4231.

Shirer, W.R., Ryali, S., Rykhlevskaia, E., Menon, V., Greicius, M.D., 2012. Decoding subject-driven cognitive states with whole-brain connectivity patterns. Cereb. Cortex 22, 158–165. https://doi.org/10.1093/cercor/bhr099.

Slobounov, S.M., Walter, A., Breiter, H.C., Zhu, D.C., Bai, X., Bream, T., Seidenberg, P., Mao, X., Johnson, B., Talavage, T.M., 2017. The effect of repetitive subconcussive collisions on brain integrity in collegiate football players over a single football season: a multi-modal neuroimaging study. Neuroimage Clin. 14, 708–718. https://doi.org/10.1016/j.nicl.2017.03.006.

Smith, S.M., Brady, J.M., 1997. SUSAN—a new approach to low level image processing. Int. J. Comput. Vis. 23, 45–78. https://doi.org/10.1023/A:1007963824710.

Stamm, J.M., Koerte, I.K., Muehlmann, M., Pasternak, O., Bourlas, A.P., Baugh, C.M., Giwerc, M.Y., Zhu, A., Coleman, M.J., Bouix, S., Fritts, N.G.M.B., Chaisson, C., McClean, M.D., Lin, A.P., Cantu, R.C., Tripodis, Y., Stern, R.A., Shenton, M.E., 2015. Age at first exposure to football is associated with altered Corpus callosum white matter microstructure in former professional football players. J. Neurotrauma 1776, 1–37. https://doi.org/10.1164/rccm.201209-1583CI.

Svaldi, D.O., Joshi, C., Robinson, M.E., Shenk, T.E., Abbas, K., Nauman, E.A., Leverenz, L.J., Talavage, T.M., 2015. Cerebrovascular reactivity alterations in asymptomatic high school football players. Dev. Neuropsychol. 40, 80–84. https://doi.org/10.1080/87565641.2014.973959.

Svaldi, D.O., McCuen, E.C., Joshi, C., Robinson, M.E., Nho, Y., Hannemann, R., Nauman, E.A., Leverenz, L.J., Talavage, T.M., 2017. Cerebrovascular reactivity changes in asymptomatic female athletes attributable to high school soccer participation. Brain Imaging Behav. 11, 98–112. https://doi.org/10.1007/s11682-016-9509-6.

Tak, S., Wang, D.J.J., Polimeni, J.R., Yan, L., Chen, J.J., 2014. Dynamic and static contributions of the cerebrovasculature to the resting-state BOLD signal. Neuroimage 84, 672–680. https://doi.org/10.1016/j.neuroimage.2013.09.057.

Tak, S., Polimeni, J.R., Wang, D.J.J., Yan, L., Chen, J.J., 2015. Associations of resting-state fMRI functional connectivity with flow-BOLD coupling and regional vasculature. Brain Connect. 5, 137–146. https://doi.org/10.1089/brain.2014.0299.

Tong, Y., Frederick, B. deB, 2010. Time lag dependent multimodal processing of concurrent fMRI and near-infrared spectroscopy (NIRS) data suggests a global circulatory origin for low-frequency oscillation signals in human brain. Neuroimage 53, 553–564. https://doi.org/10.1016/j.neuroimage.2010.06.049.

Tong, Y., Frederick, B. de B., 2012. Concurrent fNIRS and fMRI processing allows independent visualization of the propagation of pressure waves and bulk blood flow in the cerebral vasculature. Neuroimage 61, 1419–1427. https://doi.org/10.1016/j.neuroimage.2012.03.009.

Tremblay, S., Henry, L.C., Bedetti, C., Larson-Dupuis, C., Gagnon, J.-F., Evans, a.C., Theoret, H., Lassonde, M., Beaumont, L.D., 2014. Diffuse white matter tract abnormalities in clinically normal ageing retired athletes with a history of sports-related concussions. Brain 137, 2997–3011. https://doi.org/10.1093/brain/awu236.

Uddin, L.Q., Kelly, A.M.C., Biswal, B.B., Castellanos, F.X., Milham, M.P., 2009. Functional connectivity of default mode network components: correlation, Anticorrelation, and causality. Hum. Brain Mapp. 30, 625–637. https://doi.org/10.1002/hbm.20531.

Van de Moortele, P.F., Pfeuffer, J., Glover, G.H., Ugurbil, K., Hu, X., 2002. Respiration-induced Bofluctuations and their spatial distribution in the human brain at 7 tesla. Magn. Reson. Med. https://doi.org/10.1002/mrm.10145.

Viviani, R., Messina, I., Walter, M., 2011. Resting state functional connectivity in perfusion imaging: correlation maps with bold connectivity and resting state perfusion. PLoS ONE 6. https://doi.org/10.1371/journal.pone.0027050.

Wang, J., Alsop, D.C., Song, H.K., Maldjian, J.A., Tang, K., Salvucci, A.E., Detre, J.A., 2003. Arterial transit time imaging with flow encoding arterial spin tagging (FEAST). Magn. Reson. Med. 50, 599–607. https://doi.org/10.1002/mrm.10559.

Wu, W., Buxton, R.B., Wong, E.C., 2007. Vascular space occupancy weighted imaging with control of residual blood signal and higher contrast-to-noise ratio. IEEE Trans. Med. Imaging 26, 1319–1327. https://doi.org/10.1109/TMI.2007.898554.

Wu, C.W., Gu, H., Lu, H., Stein, E.A., Chen, J.H., Yang, Y., 2009. Mapping functional connectivity based on synchronized CMRO2 fluctuations during the resting state. Neuroimage 45, 694–701. https://doi.org/10.1016/j.neuroimage.2008.12.066.

Yezhuvath, U.S., Lewis-Amezcua, K., Varghese, R., Xiao, G., Lu, H., 2009. On the assessment of cerebrovascular reactivity using hypercapnia BOLD MRI. NMR Biomed. 22, 779–786. https://doi.org/10.1002/nbm.1392.

Zhang, Y., Brady, M., Smith, S., 2001. Segmentation of Brain MR Images Through a Hidden Markov Random Field Model and the Expectation-Maximization Algorithm. 20. pp. 45–57.

Zhang, X., Petersen, E.T., Ghariq, E., De Vis, J.B., Webb, A.G., Teeuwisse, W.M., Hendrikse, J., van Osch, M.J.P., 2012. In vivo blood T(1) measurements at 1.5 T, 3 T, and 7 T. Magn. Reson. Med. 000, 1–5. https://doi.org/10.1002/mrm.24550.

Zhou, Y., Milham, M.P., Lui, Y.W., Miles, L., Reaume, J., Sodickson, D.K., Grossman, R.I., Ge, Y., 2012. Default-mode network disruption in mild traumatic brain injury. Radiology 265, 882–892. https://doi.org/10.1148/radiol.12120748.

Zou, Q., Wu, C.W., Stein, E.A., Zang, Y., Yang, Y., 2009. Static and dynamic characteristics of cerebral blood flow during the resting state. Neuroimage 48, 515–524. https://doi.org/10.1016/j.neuroimage.2009.07.006.